**Current Biology, Volume *20***

# Supplemental Information

# Modulation of Bitter Taste Perception

# by a Small Molecule hTAS2R Antagonist

**Jay P. Slack, Anne Brockhoff, Claudia Batram, Susann Menzel, Caroline Sonnabend, Stephan Born, Maria Mercedes Galindo, Susann Kohl, Sophie Thalmann, Liliana Ostopovici-Halip, Christopher T. Simons, Ioana Ungureanu, Kees Duineveld, Cristian G. Bologa, Maik Behrens, Stefan Furrer, Tudor I. Oprea, and Wolfgang Meyerhof**

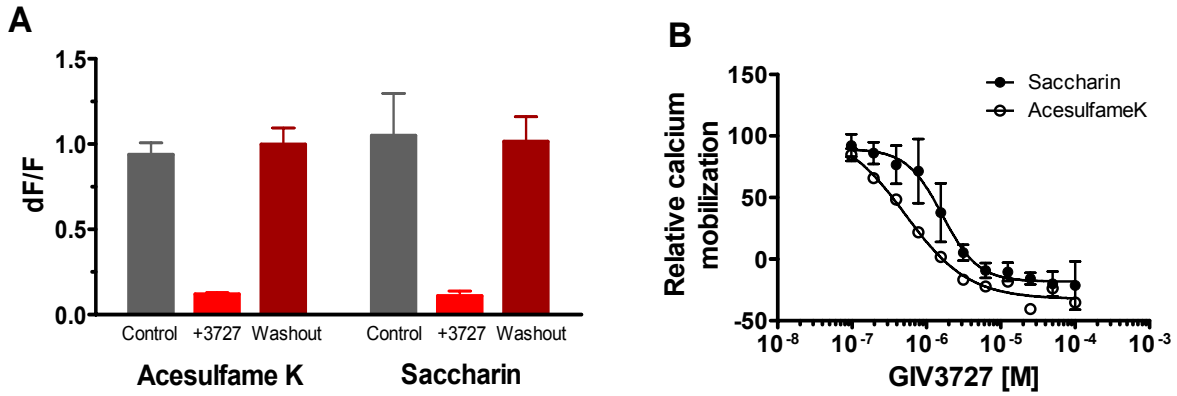


**Figure S1, Related to Figure 1.**

(A) Reversibility of GIV3727. Cells were stimulated with 500 μM sodium saccharin or 1 mM acesulfame K in the absence (gray bars) or presence (red bars) of 25 μM GIV3727. The plates were washed and then agonist alone was reapplied to cells that had been exposed to GIV3727 (dark red bars). Agonist responses following washout of GIV3727 were not different from those observed for agonist alone. Data are presented as the mean ± s.e.m. of a representative experiment performed in quadruplicate.

(B) Dose-response profile of hTAS2R43 expressing cells stimulated with either 500 μM sodium saccharin (•) or 800 μM acesulfame K (o) in the presence of increasing concentrations of GIV3727. Data are presented as the mean ± s.e.m. of two independent experiments performed in duplicate and were fitted in GraphPad Prism using a 4-parameter logistic fit equation**.**

**A**

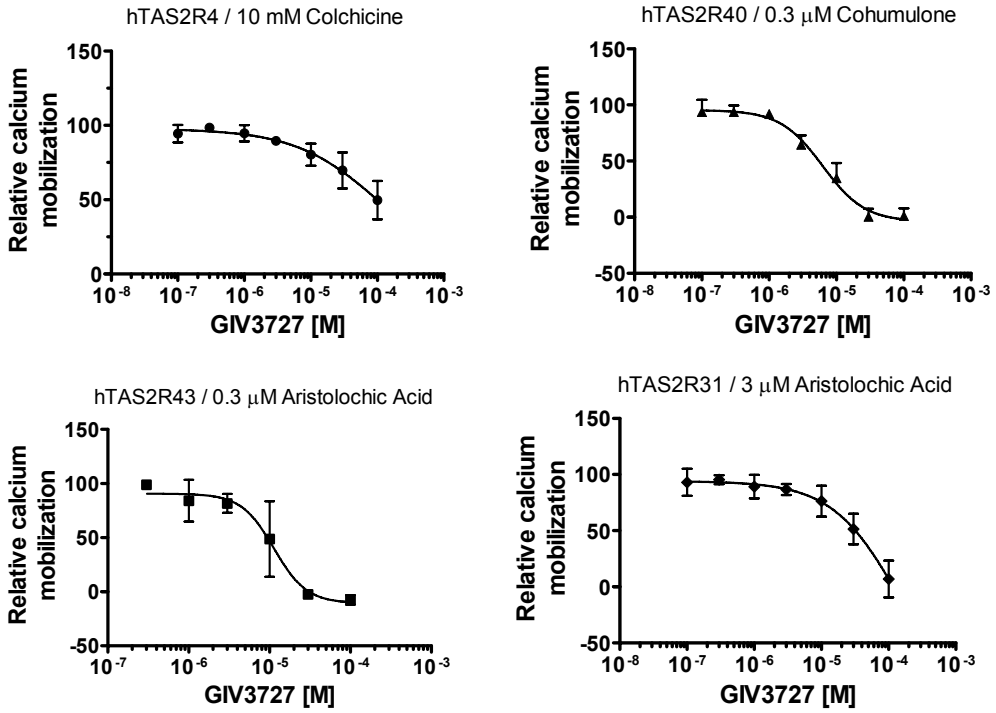


**B**

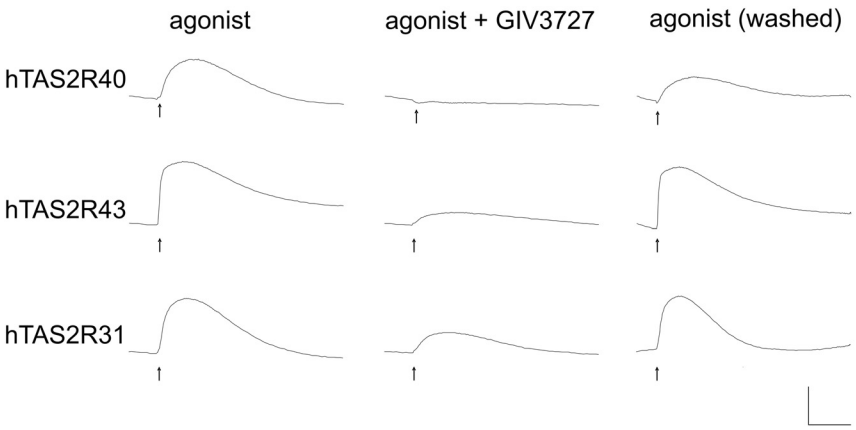


**Figure S2, Related to Table 1.**

(A) Dose-dependent inhibition of hTAS2Rs by GIV3727. $EC_{90}$ agonist concentrations were used for the cognate agonists and are indicated in the graphs. An n = 2-3 is shown for each dose-response curve, which were plotted in GraphPad Prism using a 4-parameter logistic fit equation. The data are normalized in % to the maximal signal obtained with the agonist in the absence of the inhibitor and are presented as the mean ± s.e.m. The $IC_{50}$ for GIV3727 derived from these experiments were: hTAS2R4: 108 μM; hTAS2R40: 6.24 ± 1.25 μM; hTAS2R43: 11.33 ± 2.1 μM; hTAS2R31: 34.78 ± 5.1 μM.

(B) Inhibition by GIV3727 is reversible in other hTAS2Rs. Bitter receptors were stimulated with their corresponding agonists alone (first column) or with agonist and GIV3727 (second column). After washing the cells stimulated with agonist and GIV3727, cells were washed with C1 buffer and stimulated again with the agonist (third column). For stimulations and inhibitions of the three hTAS2Rs the following substance concentrations were used: hTAS2R40 (0.3μM

cohumulone, 25µM GIV3727), hTAS2R43 (0.3µM aristolochic acid, 25µM GIV3727), hTAS2R31 (3µM aristolochic acid, 50µM GIV3727). The time points at which substances were added to the cells are indicated by arrows. Scale bar: y-axis, 3000 arbitrary light units; x-axis, 2min.

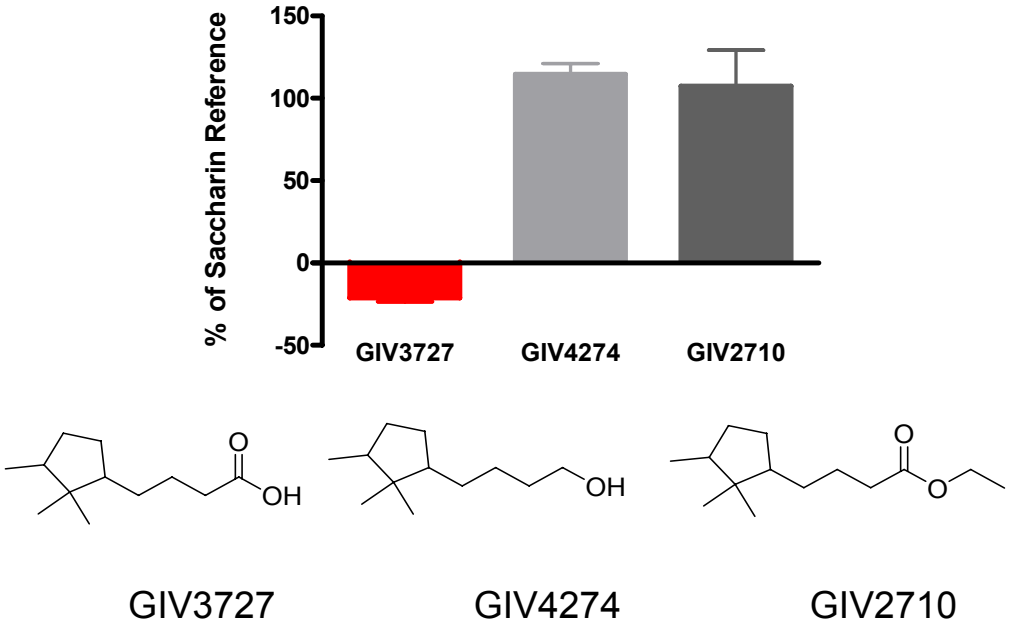


**Figure S3, Related to Figures 1 and 3.**
Elimination of the –COOH from GIV3727 abolishes inhibition of hTAS2R31. hTAS2R31 expressing cells were stimulated with 500 µM sodium saccharin in the presence of 25 µM GIV3727 and compared to activity obtained with the 25 µM of the analogous alcohol (GIV4274) or ester (GIV2710) derivatives. Data are presented as the mean ± s.e.m. of two replicates obtained in a representative experiment.

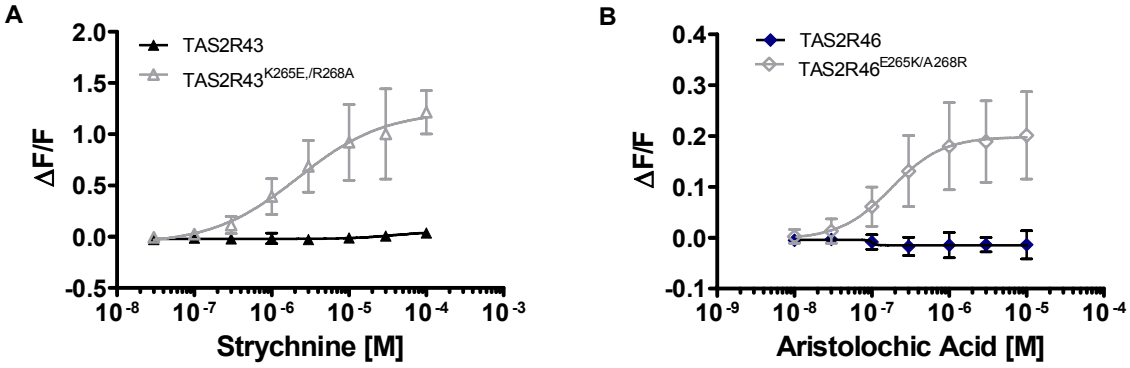


**Figure S4, Related to Figure 3.**
Site-directed mutagenesis of hTAS2R43 and hTAS2R46 reveals that $Lys^{265}/Arg^{268}$ are important for agonist specificity. Receptors were stimulated with increasing concentrations of strychnine (cognate agonist for hTAS2R46) or aristolochic acid (cognate agonist for hTAS2R43). Results are depicted above for the following constructs (A) hTAS2R43 (▲) $hTAS2R43^{K265E/R268A}$ (△) and (B) hTAS2R46 (◆); $hTAS2R46^{E265K/A268R}$ (◇) Data are presented as the mean ± s.e.m. of at least 2 independent experiments performed in duplicate and were fitted in GraphPad Prism using a 4-parameter logistic fit equation.


B

```
                        TM I                            ICL I                           TM II
2RH1     : -DEVWVVGMGIVMSLIVLAIVFGNVLVITAIAK---FERLQTVTNYFITSLACADLVMGLAVVPFGAAHILM
hTAS2R31: MTTFIPIIFSSVVVVLFVIGNFANGFIALVNSIERVKRQKISFADQILTALAVSRVGLLWVLLLNWYSTVFN

             ECL I                TM III                      ICL II           TM IV
2RH1     : KMWT--FGNFWCEFWTSIDVLCVTASIETLCVIAVDRYFAITSPFKYQSLLTKNKARVIILMVWIVSGLTSF
hTAS2R31: PAFYSVEVRTTAYNVWAVTGHFSNWLATSLSIFYLLKIANFSNL-----IFLHLKRRVKSVILVMLLGPLLF

                       ECL II                                                TM V
2RH1     : LPIQ-----MHWYRATHQEAINCYAEETCCDFFTNQAYAIASSIVSFYVPLVIMVFVYSRVFQEAKRQL---
hTAS2R31: LACQLFVINMKEIVRTKEYEGNMTWKIKLRSAVY--LSDATVTTLGNLVPFTLTLLCFLLLICSLCKHLKKM

                ICL III                 TM VI              ECL III             TM VII
2RH1     : -----KFCLKEHKALKTLGIIMGTFTLCWLPFFIVNIVHVI-QDNLIRKEVYILLNWIGYVNSGFNPLIYCR
hTAS2R31: QLHGKGSQDPSTKVHIKALQTVIFFLLLCAVYFLSIMISVWSFGSLENKPVFMFCKAIRFSYPSIHPFILIW

                    ICL IV
2RH1     : S-PDFRIAFQLLCL--------------
hTAS2R31: GNKKLKQTFLSVLRQVRYWVKGEKPSSP
```

**Figure S5, Related to the Experimental Procedures.**

(A) The AutoLigand generated best affinity fill volume (shown in green) for the hTAS2R31 receptor protein, which was used for molecular modeling.

(B) The alignment between the β2-adrenergic receptor (2RH1) and the hTAS2R31 bitter receptor. Transmembrane helices are depicted in bold. The amino acids highlighted in yellow represent the conserved residues from GPCR family present also in the bitter receptor family. Highly conserved residues in bitter receptor family but not present in hTAS2R31 receptor are depicted in gray.

**Table S1. Distribution of the Amino Acids (%) on the Ramachandran Map for hTAS2R43 and hTAS2R31 Receptors**

| | FR | AR | PA |
|---|---|---|---|
| hTAS2R43 | 93.4 | 6.6 | 0 |
| hTAS2R31 | 94.1 | 5.9 | 0 |

(FR-favored regions; AR-allowed regions; PA- prohibited areas)

**Table S2. Primers Used for Construction of hTAS2R Mutants**

| **Construct** | **Oligonucleotide** | **Sequence 5' – 3'** |
|---|---|---|
| R43 K265E R268A | R43_K265E_R268A_for | GTTCTGCGAAGCTATTGCATTCAGC |
| | R43_K265E_R268A_rev | GCTGAATGCAATAGCTTCGCAGAAC |
| R46 E265D | R46_E265D_for | CATGTTCTGCGACGCTATTGC |
| | R46_E265D_rev | GCAATAGCGTCGCAGAACATG |
| R46 E265K | R46_E265K_for | CTTCATGTTCTGCAAAGCTATT |
| | R46_E265K_rev | AATAGCTTTGCAGAACATGAAG |
| R46 E265Q | R46_E265Q_for | CATGTTCTGCCAAGCTATTGC |
| | R46_E265Q_rev | GCAATAGCTTGGCAGAACATG |
| R46 A268R | R46_A268R_for | GCTATTCGATTCAGCTATCCTTC |
| | R46_A268R_rev | GAAGGATAGCTGAATCGAATAGC |
| R46 A268G | R46_A268G_for | GCGAAGCTATTGGATTCAGCTATCC |
| | R46_A268G_rev | GGATAGCTGAATCCAATAGCTTCGC |
| **Additional Oligonucleotides** | | |
| CMV forward primer | | CTTGTCATCGTCATCCTTGTAGTCAGTTACAGTGCTG |
| BGH reverse primer | | GACTACAAGGATGACGATGACAAGTATCAGTTCCAGGC |

**Table S3. For the Single Point Mutant Studies Presented in Figure 3c, the Following Constructs, Ligands and Concentrations Were Used**

| Construct | Ligand / Concentration | Signal Amplitude (dF/F) |
|---|---|---|
| hTAS2R46 | 3 μM strychnine | 0.38 |
| hTAS2R46-E265K/A268R | 0.3 μM aristolochic acid | 0.16 |
| hTAS2R46-E265K | 100 μM strychnine | 0.11 |
| hTAS2R46-E265Q | 100 μM strychnine | 0.26 |
| hTAS2R46-E265D | 30 μM strychnine | 0.29 |
| hTAS2R46-A268R | 100 μM strychnine | 0.10 |
| hTAS2R46-A268G | 3 μM strychnine | 0.24 |

Also shown are the maximal signal amplitudes obtained following receptor activation by the agonists.

**Supplemental Experimental Procedures**

**Chemical Synthesis of GIV3727**

***Synthesis Scheme for GIV3727***

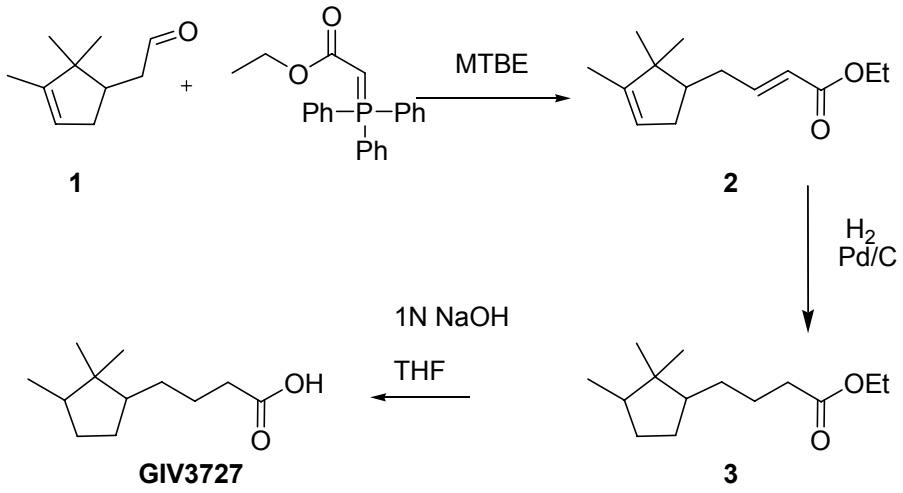


***Ethyl 4-(2,2,3-trimethylcyclopent-3-enyl)but-2-enoate*** **(2)**

A 300-mL round-bottomed flask equipped with a magnetic stir bar and flushed with nitrogen was charged with campholenic aldehyde (**1**, 10.0 g, 65.7 mmol) in 100 ml of MTBE and the solution was cooled to 0°C. (Carbethoxymethylene)triphenyl-phosphorane (22.8 g, 66.0 mmol) was slowly added to the solution. The reaction mixture was stirred at 0°C for 20 min then at room temperature for 24 h. After the completion (TLC), the reaction mixture was reduced to half its volume under vacuum and 100 ml of hexanes were added. The mixture was cooled in an ice bath for 30 min then filtered through a plug of celite, silica and sand. The plug was washed three times with hexanes/MTBE. The combined organic fractions were concentrated and the crude material was purified *via* flash column chromatography (1:8 Hexanes/AcOEt) to give ethyl 4-(2,2,3-trimethylcyclopent-3-enyl)but-2-enoate (**2**, 13.1 g, 89%) as a colorless oil.
$^{1}$H NMR (300 MHz, CDCl3) δ 6.92 (dd, *J* = 10.5, 7.5 Hz, 1H), 5.79 (d, *J* = 15.6 Hz, 1H), 5.13 (s, 1H), 4.13 (m, 2H), 2.3 (m, 2H), 2.1 (m, 1H), 1.8 (m, 2H), 1.52 (s, 3H), 1.24 (t, *J* = 15, 3H), 0.91 (s, 3H), 0.71 (s, 3H) ; $^{13}$C NMR (75 MHz, CDCl3) δ 166.1, 148.6, 147.8, 121.5, 121.3, 59.6, 48.9, 46.2, 35.2, 32.9, 25.5, 19.5, 14.0, 12.2; MS *m/z* 222.

***Ethyl 4-(2,2,3-trimethylcyclopentyl)butanoate*** **(3)**

A 300-mL three-necked round-bottomed flask equipped with a magnetic stir bar and flushed with nitrogen was charged with Degussa type palladium on charcoal Pd/C (1.5 g, 10% Pd) and distilled water (8 ml). A solution of ethyl 4-(2,2,3-trimethylcyclopent-3-enyl)but-2-enoate (**2**, 10.0 g, 44.9 mmol) in AcOEt (200 ml) was added and the flask was flushed with hydrogen. The reaction was run under hydrogen balloons that were refilled as needed. After 17 h at room temperature the reaction was found to be completed by GCMS. The reaction mixture was filtered through a celite plug, the organic phase concentrated under vacuum and purified *via* flash

column chromatography using a gradient of AcOEt/ Hexanes to give ethyl 4-(2,2,3-trimethylcyclopentyl)butanoate as a colorless oil (**3**, 7.48 g, 74%).
$^{1}$H NMR (300 MHz, CDCl3) δ 4.18 (q, *J* = 7.14, 2H), 2.34 (m, 2H), 1.82 (m, 3H), 1.56 (m, 5H), 1.30 (t, *J* =7.2 , 3H), 1.21 (m, 2H), 0.99 (s, 3H), 0.86 (d, *J* = 5.4, 2H), 0.52 (s, 3H); $^{13}$C NMR (75 MHz, CDCl3) δ 173.8, 60.1, 50.6, 45.2, 42.2, 34.8, 30.1, 30.0, 28.1, 25.6, 24.3, 14.3, 14.2, 13.8; MS *m/z* 226.

***4-(2,2,3-trimethylcyclopentyl)butanoic Acid*** **(GIV3727)**

A 100 mL round-bottomed flask equipped with a magnetic stir bar and fitted with a condenser was charged with a solution of ethyl 4-(2,2,3-trimethylcyclopentyl)butanoate (**3**, 5 g, 22 mmol) in THF (25 ml) and an aqueous solution of 1N NaOH (25 ml). The reaction mixture was refluxed at 110° C for 8 h. Upon completion, the reaction mixture was diluted with 1 N NaOH (25 ml) and the aqueous layer washed with MTBE (50 ml x 2) then acidified (pH=4) with aqueous 1N HCl and extracted with AcOEt (50 ml x 3). The combined organic layers were concentrated under vacuum and purified *via* flash column chromatography with to give 4-(2,2,3-trimethylcyclopentyl)butanoic acid (**GIV3727**) as a colorless oil (3.82 g, 87%).
1H NMR (300 MHz, CDCl3) δ 11.22 (br s, 1H), 2.37 (m, 2H), 1.75 (m, 3H), 1.49 (m, 4H), 1.17 (m, 3H), 0.86 (s, 3H), 0.84 (d, J = 6.9 Hz, 3H), 0.52 (s, 3H); $^{13}$C NMR (75 MHz, CDCl3) δ 179.9, 50.6, 45.2, 42.2, 34.4, 30.1, 30.0, 28.1, 25.0, 24.0, 14.3, 13.8; MS m/z 198.

**Functional Expression of hTAS2Rs**

Human TAS2R cDNA constructs were used that encoded a plasma membrane-targeting sequence of the rat somatostatin type 3 receptor (sst3) at the N terminus of the recombinant polypeptide and a herpes simplex virus glycoprotein D (hsv) epitope at its C terminus, as previously reported [1]. The constructs were transiently transfected into human embryonic kidney HEK293T cells that stably express the chimeric G-protein subunit $G_{\alpha 16gust44}$ [2] using Lipofectamine 2000 (Invitrogen, San Diego, CA). They were then seeded at a density of 70,000 ± 10,000 per well in 96-well microtiter plates. Calcium imaging experiments using an automated fluorometric imaging plate reader (FLIPR) (MolecularDevices) were performed 24–32 hr post-transfection essentially as described previously [1]. Tastants were dissolved and administered in assay buffer (in mM): 130 NaCl, 5 KCl, 10 HEPES, 2 $CaCl_2$, and 10 glucose, pH 7.4. Transiently transfected cells were challenged with tastant and compared to vehicle alone and/or mock transfected cells, Data were collected from a minimum of three independent experiments performed with 2-4 replicates and processed with GraphPad Prism version 5.0 (GraphPad Software, San Diego CA). For dose–response curve calculations, the peak fluorescence responses after compound addition were corrected for and normalized to background fluorescence (ΔF/F = (F - F0)/F0), and baseline noise was subtracted.

**Stable Cell Line Generation**

Stable cell lines for hTAS2R43 and hTAS2R31 were generated by subcloning the sst3:TAS2R:hsv cassette into pcDNA3.1-Zeo (Invitrogen, San Diego CA) and the resulting construct was linearized and transfected into the $G_{\alpha 16gust44}$/HEK293T host cells. After 48 hours post-transfection, the cells were treated with 200 μg/ml Zeocin (Invivogen, San Diego CA) to

select for stable transfectants. After 2-4 weeks, zeocin-resistant colonies were selected, expanded and clones expressing hTAS2R43 or hTAS2R31 were identified based on a robust response to 5 mM saccharin and 5 mM acesulfame K.

**High-Throughput Screening for hTAS2R31 Antagonists**

On Day 0, the hTAS2R31 cell line was pre-plated at a density of 15,000 cells per well in DMEM + 10% FBS in black, clear bottom 96-well plates that had been pre-coated with 0.001 % poly(ethyleneimine) (MW = ~60,000, Acros Organics, Morris Plains, NJ). On day 2, high-throughput screening of antagonists was performed via calcium imaging using Fluo-4. Briefly, growth medium was discarded and the cells were incubated in the dark for 1 hour at 37° C in 50 µl loading buffer consisting of 1.5 µM Fluo-4 AM (Invitrogen, San Diego CA) and 2.5 µM probenicid (Sigma-Aldrich, St. Louis, MO, US) in DMEM (no FBS). After incubation, the plates were washed 5X with 100 µl of assay buffer (described above) and further incubated in the dark at room temperature for 30 minutes. The cells were then washed 5X with 100 µl assay buffer and then calcium responses were measured in a FLIPR$^{TETRA}$ (Molecular Devices, Sunnydale, CA). Test compounds were prepared at a final concentration of 25 µM in the presence of an $EC_{50}$ concentration of saccharin (500 µM) and assessed for their ability to decrease the hTAS2R31 response to saccharin. Putative hits that showed >50% inhibition of the saccharin response during primary screening were selected and retested for their ability to inhibit hTAS2R31 activation by saccharin as well as acesulfame K. Hits that also caused a decrease in the agonist responses of a non-related GPCR pathway (isoproterenol, $\beta_1/\beta_2$-adrenergic receptor agonist) were considered as non-specific inhibitors.

**Molecular Modeling**

The sequences of the human TAS2R43 and hTAS2R31 have been automatically aligned with the sequence of the human $\beta_2$-adrenergic receptor ($\beta_2$-AR) using the T-coffee server [3, 4]. The resulting alignment was then manually refined according to the three dimensional structure of the template, in order to preserve the highly-conserved amino acid motifs specific for each transmembrane helix [5]. The final alignment was used as input to generate the three-dimensional structures for hTAS2R43 and hTAS2R31 receptors using the SWISS_MODEL server [6, 7]. Finally, the models were refined to reduce the steric clashes of the side chains without changing the receptor backbone. Docking was carried out with AutoDock4.0 software [8, 9]. The grid box was centered on $Lys^{265}$ and set at 20Åx20Åx20Å, with a spacing of 0.375 Å between grid points. In a preliminary run, the grid box was chosen to embed the entire protein and one affinity map for each atom type included in the receptor was generated. In the following runs, the grid was defined around the main active site cavity identified with AutoLigand [10, 11] (Figure S5A). Receptors and ligands were prepared by adding the polar hydrogens and by applying the ionization states at physiological conditions. Kollman united atom charges have been calculated for the receptors and Gasteiger-Marsili atomic partial charges for the ligands

***Sequence Alignment***

The sequences of the human bitter receptors were extracted from the SWISS-Prot databank in Fasta format and automatically aligned with the sequences of the following GPCRs with known

crystal structures: bovine rhodopsin [12] (PDB accession code: 1U19), human $\beta_2$-adrenergic receptor [13] (PDB accession code: 2RH1), turkey $\beta_1$-adrenergic receptor [14] (PDB accession code: 2vt4) and squid rhodopsin [15] (PDB accession code: 2Z73). The output was further refined manually in order to avoid deletions or insertions in the alpha helices and to preserve the conserved amino acid patterns in the transmembranes. As we expected, part of the conserved residues in the transmembrane helices were not present in the bitter receptors but despite this fact we were still able to find markers for each important region of the receptor (yellow residues in figure S5B). This operation was repeated for each 3D crystal structure, and if necessary, the deletions and insertions were merged into a single piece per loop and placed in the most adequate point of the template structure. Using ClustalW software [16] a phylogenetic tree was generated based on the final sequence alignment. Based on the evolutionary relationships among bitter receptors and template structures as well as on sequence similarity, the most appropriate template for homology modeling of hTAS2R43 and hTAS2R31 structures was found to be the crystal structure of human $\beta_2$ adrenergic receptor (PDB accession code: 2RH1; 37% sequence similarity).

***Homology Modeling***

The SWISS-MODEL server [6, 7] was used to generate the three-dimensional models for hTAS2R43 and hTAS2R31. The C- and N-termini were not modeled. The resultant models were refined with the Biopolymer module from Sybyl (SYBYL 7.3, Tripos International) in order to reduce the steric clashes of the side chains without changing the receptor backbone. The final models have over 90% of residues in the favorable regions of the Ramachandran map and all the main-chain parameters like peptide bond planarity, bad non-bonded interactions, Cα distortion, overall G-factor, bond length distribution and side-chain parameters are in the normal range (see Supplementary Table 1).

***Docking***

Docking was carried out with AutoDock4.0 software [8, 9] by combining a rapid energy evaluation through precalculated grids of affinity potentials with a Lamarckian algorithm to find a suitable binding position for the ligand. The most favorable binding site was identified with AutoLigand, which rapidly scans the protein surface for high-affinity binding pockets. In this process, a flood-fill of the input volume is accomplished and then the fill volumes migrate to find the shape and the location with the best binding energy. The search stops when a better solution cannot be found during the points' migration. The most favorable site of the hTAS2R31 receptor is shown in Figure S5A. The grid box was centered on Lys265 and set at 20Åx20Åx20Å, with a spacing of 0.375 Å between grid points. Docking was performed by applying a standard protocol, with a initial population of 150 randomly placed individuals, a maximum number of $2.5x10^6$ energy evaluations, a mutation rate of 0.02, a crossover rate of 0.8, and a elitism value of 1. Ten independent docking runs were performed for each ligand. Results differing by less than 0.5Å in positional root-mean-square deviation (rmsd) were clustered together and represented by the result with the most favorable free energy of binding.

## Generation of Mutant hTAS2R Constructs

The influence of distinct amino acid residues on the sensitivity of hTAS2R43 and hTAS2R46 for GIV3727 was investigated by using mutated hTAS2R constructs available from a previous study (Brockhoff et al., in review). Recombinant hTAS2R cDNAs were generated by site-directed mutagenesis using a two-step PCR protocol. First, two subfragments were mutated and amplified from the template cDNA. Primers used for these studies are listed below in the Supplementary Table. Briefly, the 5' fragments for mutants were created by using the vector-specific CMV forward primer along with the mutation-specific reverse mutagenesis primer. The 3' fragments were obtained with the vector-specific BGH reverse primer and the mutant-specific forward mutagenesis primer. PCR conditions were: 5 min 95°C; 15 cycles: 1 min annealing (equation for calculation of annealing temperatures: T≈ Tmelt-3°C-(3°C*mismatching bp)), 0.5-2.5 min 72°C, 30 sec 95°C; 5 min annealing; 10 min 72°C. Second, the purified subfragments were recombined and amplified with CMV forward and BGH reverse primer. PCR conditions were: 5 min 95°C; 15 cycles: 2 min 54°C, 3 min 72°C, 30 sec 95°C; 5 min 54°C; 10 min 72°C. The purified fragments were subcloned into pcDNA5/FRT-sst3-MCS-hsv to provide an amino terminal sst-tag and a carboxy terminal hsv-tag to the receptor constructs. All constructs were verified by DNA sequencing.

## Human Psychophysics Determinations

GIV3727 has been approved for use in foods and beverages after receiving the GRAS designation (Generally Recognized As Safe) under the Food Additives Amendment to the U.S. Federal Food, Drug, and Cosmetic Act [17, 18] and the GRAS identification number for this molecule is 4529. Sensory protocols to assess the effects of GIV3727 on taste perception were administered in test subjects with informed written consent and after prior approval by the Givaudan Institutional Review Board. For 2-alternative forced choice measurements (2-AFC), twenty milliliters each of acesulfame K (2 mM) and acesulfame K + GIV3727 (30 ppm) were presented in random order at room temperature to 22 subjects that had been pre-identified as sensitive to the bitterness of the sulfonamides given that this trait varies in humans (see reference 25 in main paper). Over two trials (with a 5 min break between reps) panelists were asked to select the solution perceived as being most bitter (trial 1) or as most sweet (trial 2). After the first trial, the panelists were asked to rate the perceived bitter taste intensity of both solutions using a 0-100 line scale with anchors at the following intervals: 0 = no bitterness, 25 = recognizable, 50 = moderate, 75 = strong, 100 = extreme. In the second trial, panelists were asked to rate the perceived sweet taste intensity of the two solutions following selection of the sample that was most sweet. To determine if a significant number of panelists identified the sample without the antagonist as being most bitter or sweet, a binomial analysis was used. ANOVA was used to determine whether perceived taste intensity ratings were statistically different between the samples. A $p < 0.05$ was taken as significant in both statistical tests. In separate sessions, 15 panelists evaluated the effect of GIV3727 (30 ppm) on sodium saccharin solutions (3 mM), using the same 2-AFC procedure but without the taste intensity ratings. Each panelist performed two replicates of the test. The results from the sodium saccharin studies were analyzed using beta-binomial statistics and corrected for possible over dispersion in the data. Finally, 30 ppm GIV3727 was examined via triangle test for intrinsic taste or aroma properties that would render it identifiable from a water reference. Briefly, three samples were presented

simultaneously to each panelist. Two samples were identical and one was different (odd). Samples were served to the panelists in a balanced, randomized order. Panelists were asked to evaluate the samples from left to right and select the odd sample. A significance level of $p=0.05$ was set following binomial statistical analysis.

**Author Contributions**

J.P.S conceived of the project, supervised HTS screening for TAS2R inhibitors, performed the mechanism studies for GIV3727 and drafted the manuscript with input from all authors. A.B., C.B., S.M., C.S., S.B., M.M.G., S.K., and M.B. performed the *in vitro* transfection experiments using wild-type and mutant hTAS2Rs. C.T.S. and K.D. were responsible for all psychophysical testing. C.G.B. and L.O-H. performed the molecular modeling studies, while T.I.O. and S.F. provided intellectual input to scientific direction and interpretations. I.U. performed chemical synthesis and analysis of GIV3727 and its derivatives. W.M. contributed to the design of the study, supervised the *in vitro* transfection experiments and provided interpretations for many of the experimental results.

**Supplemental References**


1. Bufe, B., Hofmann, T., Krautwurst, D., Raguse, J.-D., and Meyerhof, W. (2002). The human TAS2R16 receptor mediates bitter taste in response to β-glucopyranosides. Nat Genet *32*, 397-401.
2. Ueda, T., Ugawa, S., and Shimada, S. (2005). Functional interaction between TAS2R receptors and G-protein alpha subunits expressed in taste receptor cells. Chem Senses *30 Suppl 1*, i16.
3. Notredame, C., Higgins, D.G., and Heringa, J. (2000). T-coffee: a novel method for fast and accurate multiple sequence alignment. J Mol Biol *302*, 205-217.
4. Poirot, O., O'Toole, E., and Notredame, C. (2003). Tcoffee@igs: a web server for computing, evaluating and combining multiple sequence alignments. Nucl Acids Res *31*, 3503-3506.
5. Baldwin, J.M., Schertler, G.F.X., and Unger, V.M. (1997). An alpha-carbon template for the transmembrane helices in the rhodopsin family of G-protein-coupled receptors. J Mol Biol *272*, 144-164.
6. Arnold, K., Bordoli, L., Kopp, J., and Schwede, T. (2006). The SWISS-MODEL workspace: a web-based environment for protein structure homology modelling. Bioinformatics *22*, 195-201.
7. Schwede, T., Kopp, J., Guex, N., and Peitsch, M.C. (2003). SWISS-MODEL: an automated protein homology-modeling server. Nucl Acids Res *31*, 3381-3385.
8. Goodsell, D.S., Morris, G.M., and Olson, A.J. (1996). Automated docking of flexible ligands: Applications of autodock. J Mol Recognit *9*, 1-5.
9. Morris, G.M., Goodsell, D.S., Halliday, R.S., Huey, R., Hart, W.E., Belew, R.K., and Olson, A.J. (1998). Automated docking using a Lamarckian genetic algorithm and an empirical binding free energy function. J Comput Chem *19*, 1639-1662.
10. Harris, R., Olson, A.J., and Goodsell, D.S. (2008). Automated prediction of ligand-binding sites in proteins. Proteins *70*, 1506-1517.

11. Sanner, M.F. (1999). Python: a programming language for software integration and development. J Mol Graph Model *17*, 57-61.
12. Okada, T., Sugihara, M., Bondar, A.-N., Elstner, M., Entel, P., and Buss, V. (2004). The retinal conformation and its environment in rhodopsin in light of a new 2.2 A crystal structure. J Mol Biol *342*, 571-583.
13. Cherezov, V., Rosenbaum, D.M., Hanson, M.A., Rasmussen, S.G.F., Thian, F.S., Kobilka, T.S., Choi, H.-J., Kuhn, P., Weis, W.I., Kobilka, B.K., et al. (2007). High-resolution crystal structure of an engineered human $\beta_2$-adrenergic G protein coupled receptor. Science *318*, 1258-1265.
14. Warne, T., Serrano-Vega, M.J., Baker, J.G., Moukhametzianov, R., Edwards, P.C., Henderson, R., Leslie, A.G.W., Tate, C.G., and Schertler, G.F.X. (2008). Structure of a $\beta_1$-adrenergic G-protein-coupled receptor. Nature *454*, 486-491.
15. Murakami, M., and Kouyama, T. (2008). Crystal structure of squid rhodopsin. Nature *453*, 363-367.
16. Larkin, M.A., Blackshields, G., Brown, N.P., Chenna, R., McGettigan, P.A., McWilliam, H., Valentin, F., Wallace, I.M., Wilm, A., Lopez, R., et al. (2007). Clustal W and Clustal X version 2.0. Bioinformatics *23*, 2947-2948.
17. Hallagan, J.B., and Hall, R.L. (1995). FEMA GRAS - A GRAS Assessment Program for Flavor Ingredients. Regul Toxicol and Pharmacol *21*, 422-430.
18. Hallagan, J.B., and Hall, R.L. (2009). Under the conditions of intended use - New developments in the FEMA GRAS program and the safety assessment of flavor ingredients. Food Chem Toxicol *47*, 267-278.